J. Korean Earth Sci. Soc., v. 45, no. 4, p. 318–326, August 2024
https://doi.org/10.5467/JKESS.2024.45.4.318
ISSN 1225-6692 (printed edition)
ISSN 2287-4518 (electronic edition)

# Preliminary Study on Black-Ice Detection Using GPS Ground Reflection Signals

**Young-Joo Kwon[1], Hyun-Ju Ban[2], Sumin Ryu[3], Suna Jo[2], Han-Sol Ryu[2], Yerin Kim[2], Yun-Jeong Choi[2], and Sungwook Hong[2,*]**

[1]Moon Soul Graduate School of Future Strategy, Korea Advanced Institute of Science and Technoogy, Daejeon 34141, Republic of Korea
[2]Department of Environment, Energy, and Geoinformatics, Sejong University, Seoul 05006, Republic of Korea
[3]Satellite Application Division, Korea Aerospace Research Institute, Daejeon 34133, Republic of Korea

**Abstract:** Black ice, a thin and nearly invisible ice layer on roads and pavements, poses a significant danger to drivers and pedestrians during winter due to its transparency. We propose an efficient black ice detection system and technique utilizing Global Positioning System (GPS)-reflected signals. This system consists of a GPS antenna and receiver configured to measure the power of GPS L1 band signal strength. The GPS receiver system was designed to measure the signal power of the Right-Handed Circular Polarization (RHCP) and Left-Handed Circular Polarization (LHCP) from direct and reflected signals using two GPS antennas. Field experiments for GPS LHCP and RHCP reflection measurements were conducted at two distinct sites. We present a Normalized Polarized Reflection Index (NPRI) as a methodological approach for determining the presence of black ice on road surfaces. The field experiments at both sites successfully detected black ice on asphalt roads, indicated by NPRI values greater than –0.1 for elevation angles between 45° and 55°. Our findings demonstrate the potential of the proposed GPS-based system as a cost-effective and scalable solution for large-scale black ice detection, significantly enhancing road safety in cold climates. The scientific significance of this study lies in its novel application of GPS reflection signals for environmental monitoring, offering a new approach that can be integrated into existing GPS infrastructure to detect widespread black ice in real-time.

Keywords: Black ice, GPS, Polarization, Reflection, Remote sensing

## 1. Introduction

In many northern countries that experience freezing and thawing, serious traffic accidents occur every winter. Such fatal traffic accidents are related to slippery road conditions, such as icy or snowy road surfaces. In particular, black ice, which is a transparent ice layer on surfaces, is dangerous for both drivers and pedestrians (Chapman and Thornes, 2011; Norrman et al., 2000). Owing to its high transparency, black ice can create unexpected situations that may lead to accidents. To reduce this accident risk, we need information about road surface status depending on the prevailing weather conditions.

However, existing sensors and systems (Chapman and Thornes, 2011; Mahoney and Myers, 2003; Pilli-Sihvola et al., 2006) have difficulty detecting the presence of ice or frost on surfaces near the freezing temperature of water. Conductivity-based ice sensors (Liu et al., 2017), which estimate conditions for ice formation by measuring temperature and humidity, are highly accurate in detecting ice. However, they pose challenges due to the complexity of sensor management and limited area coverage. Black ice detection methods using IR (Jonsson, 2011; Nakanishi and Kushihi, 2021) and optical sensors (Ma and Ruan, 2020; Alimasi et al., 2012) exploit the difference in absorption coefficients between water and ice depending on the incident radiation. While these methods provide

*Corresponding author: sesttiya@sejong.ac.kr; sesttiya@gmail.com
Tel: +82-2-6935-2430

accurate ice detection, they are limited by their susceptibility to sunlight interference and high costs. These sensors also struggle to differentiate between black ice and wet surfaces due to similar temperature readings. High-resolution camera systems are often expensive and require complex calibration and maintenance. Additionally, they are generally affected by low-light conditions (Najafi et al., 2024).

The distinctive reflection characteristics of water and ice in the microwave region can be a good alternative to solve this problem. In the microwave spectral bands, the reflectance of water is much higher than that of ice, especially in L-band microwaves (Johnson et al., 2012). Using this difference in reflectivity, the state of the road surface i.e. whether it is covered in water or ice, can be determined. Furthermore, the main frequencies of Global Navigation Satellite System (GNSS) satellites are L-band microwaves.

The GNSS has been developed for accurate estimation of geodetic point position (i.e., longitude, latitude, and elevation). This term includes the Global Positioning System (GPS) in the United States, the Russian GLONASS, the European Galileo, and the Chinese COMPASS (Beidou). Among them, GPS is the most utilized navigation system based on satellites for exceptionally precise position tracking. A total of 32 GPS satellites have launched by the United States since 1978, and now 24 satellites are operational in orbit. The altitude of the satellites is about 20,180 km. There are six orbits, and each orbit has four satellites with intervals of $60^{o}$. This GPS orbital arrangement allows observations of the ground by 5-8 satellites. GPS satellites broadcast signals at two L-band frequencies of 1.57542 GHz (L1 band) and 1.2276 GHz (L2 band) (Parkinson and Spilker, 1996).

Over the last two decades, GPS has been applied in not only geodynamics but also in various geophysical studies. GPS has been employed to measure integrated water vapor (Bevis et al., 1992) or precipitable water vapor (Choy et al., 2015) using time delay due to water vapor in the atmosphere. GPS interferometric reflectometry technique has been used to measure soil moisture (Larson et al., 2008), snow depth (Larson et al., 2009), vegetation water content (Larson and Small, 2014; Evans et al., 2014), and sea ice conditions (Komjathy et al., 2000). Larson (2016) summarized these successful applications of GNSS reflectometry. Recently, Koch et al. (2016) suggested a new method to retrieve soil moisture in bare soil of 0-10 cm depth using two GPS receive antennas.

The L1 and L2 band of GPS signals are more sensitive to various land surface materials such as water and soil (Njoku and Entekhabi, 1996). The aim of our research is to apply these reflectivity characteristics to enable the detection of black ice. In this work, we tested the possibility of detecting black ice using the strength of reflected GPS signals of L1 band.

## 2. Data

We developed a GPS receiver module for the measurement of GPS signal strength. The module was designed to simultaneously receive direct and reflected GPS L1 signals. This module can be roughly divided into three parts: antenna, radio frequency (RF) front-end board, and GPS signal processing board. We used two commercial antennas (dual-polarization L1/L2 GNSS antenna of Antcom) and a U-Blox M8T Evaluation Kit. For the automatic storage and extraction of data, we developed a python code to automatically save NMEA-0183 protocol to files, from 3 U-Blox serial ports. The procedure for acquiring received GPS signals was controlled by Raspberry Pi, a low-cost acquisition system with embedded Linux. The concept of the GPS reflectance receiver module for black-ice detection is illustrated in Fig. 1.

The GPS reflection measurement experiments were performed at two different sites. The first experimental site was the Ttukseom Han River Park in Seoul (November 16, 2016), hereafter referred to as experiment A. This observation site had a sandy soil surface. Firstly, we measured the strength of direct and reflected GPS signals, and then we sprayed water onto the soil surface for about 45 min to examine changes in reflectivity. The air temperature, wind speed, and relative humidity were $4.7^{o}$C, 0.8 m/s, and 43%, respectively.

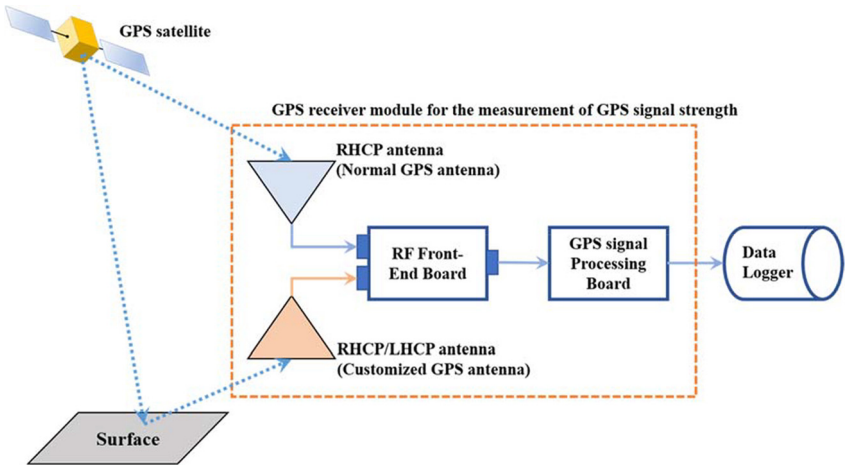


**Fig. 1.** GPS reflectance receiver module for black ice detection.

The second experiment was performed at a public service garage for trucks in Chuncheon (November 24, 2016), hereafter referred to as experiment B. The air temperature, wind speed, and relative humidity under clear sky condition were −3.3°C, 1.3 m/s, and 64%, respectively. The direct and reflected GPS signals on different ground surfaces of asphalt and ice were repeatedly measured at intervals of 30 min. In both experiments, the antenna height was maintained at about 25 cm. Table 2 summarizes the GPS signal reflection experiments in this study.

## 3. Methods

GPS satellites transmit signals in right-hand circular polarization (RHCP, Parkinson and Spilker, 1996). Upon reflection from surfaces, the transmitted RHCP wave can transform into both RHCP and left-hand circular polarization (LHCP) components (Zavorotny and Voronovich, 2000). The Fresnel equations describe the fundamental properties of reflectance from a specular surface. The reflection coefficients employed in this study are as follows (Hong (2009, 2013)):

$$r_V(\theta) = \frac{\cos\theta - \sqrt{N^2 - \sin^2\theta}}{\cos\theta + \sqrt{N^2 - \sin^2\theta}} \quad (1)$$

$$r_H(\theta) = \frac{N^2\cos\theta - \sqrt{N^2 - \sin^2\theta}}{N^2\cos\theta + \sqrt{N^2 - \sin^2\theta}} \quad (2)$$

where $\theta$ represents the incidence angle, $N$ denotes complex refractive index in the form of $N = n + ik$ ($i = \sqrt{-1}$). Here, $n$ and $k$ are the real and imaginary parts of the refractive indices, respectively. The reflectance over specific surfaces is contingent on the incident angle, and refractive index (or dielectric constants) of the reflecting medium. For instance, the reflectivity of water is significantly higher than that of ice in the L1 and L2 bands of GPS satellite signals (Fig. 2a). The reflectance of the specular surface in polarized microwave has a relationship with the reflection coefficient: $R_p = |r_p|^2$ for p-polarization, where $p$ means vertical (V) or horizontal (H) polarization. The complex reflective coefficients, $r_V$ for vertical polarization and $r_H$ for horizontal polarization, can be expressed as circular components of the two orthogonal polarizations as follows:

$$R_{RR} = \left|\frac{r_V + r_H}{2}\right|^2 \quad (3)$$

$$R_{RL} = \left|\frac{r_V - r_H}{2}\right|^2 \quad (4)$$

where $R_{RR}$ means reflectance of the circularly polarized electromagnetic wave from RHCP to RHCP (co-polarized reflectance). Similarly, $R_{RL}$ signifies the reflectance from RHCP to LHCP (cross-polarized reflectance).

To calculate the reflectance of the specular surface

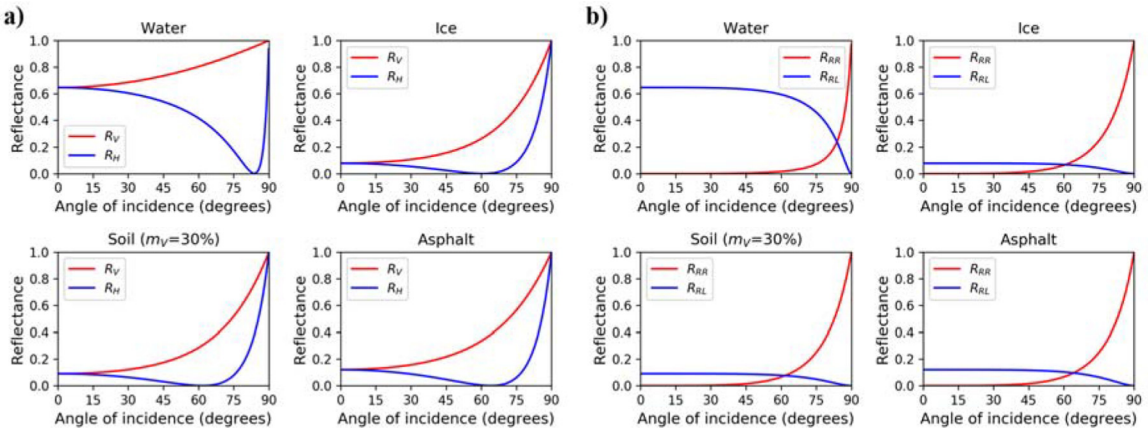


**Fig. 2.** Reflectance of a specular surface for different media: water, ice, soil, and asphalt. (a) Reflectance for vertical ($R_V$) and horizontal ($R_H$) polarization; (b) Co-polarized reflectance ($R_{RR}$) and cross-polarized reflectance ($R_{RL}$).

using equation (3) and (4), the refractive indices are required. The real and imaginary parts of the refractive index are related to the complex permittivity ($\varepsilon_r = N^2 = (n + ik)^2$, which is assumed to be a modified Debye-type relaxation. The complex permittivity ($\varepsilon_r = \varepsilon' + i\varepsilon''$) of a medium is characterized by the relaxation time and the static dielectric constants for a given frequency and temperature. Various dielectric constant models for the low-frequency range (1-20 GHz) have been developed for each material type. We utilized the refractive indices converted from complex permittivity obtained from dielectric constant models for different surface types: water, ice, soil and asphalt. The dielectric constants and relevant information for each medium are summarized in Table 1. Figure 2a shows the reflectance of vertical ($R_V$) and horizontal ($R_H$) polarization for different media. Similarly, Figure 2b illustrates the co-polarized (from RHCP to RHC signal) and cross-polarized (from RHCP to LHCP signal) reflectance.

**Table 1.** Refractive index and dielectric constant models for each material

| Medium | n | k | Reference |
|---|---|---|---|
| Water | 9.189 | 0.635 | Stogryn (1971) |
| Ice | 1.775 | 0.0001 | Hufford (1991) |
| Soil ($m_v$ = 30%) | 1.857 | 0.0281 | Dobson et al. (1985) |
| Asphalt | 2.062 | 0.024 | Piuz i et al. (2016) |

The quantity measurement of GPS signal power can be evaluated as signal-to-noise ratios (SNR) on the reflected and on the direct signal, respectively. We assumed that the direct GPS transmitted signal power ($SNR_{RHCP}$) is dominant for the upward GPS antenna and reflected RHCP ($SNR_{RR}$) and LHCP ($SNR_{RL}$) signals are dominant for downward antenna. The SNR of the direct and reflected signal power can be expressed as follows:

$$SNR_{RHCP} = P_{in}\frac{G_R}{N_{sys}} \tag{5}$$

$$SNR_{RL} = P_{in}R_{RL}\exp\left[-\left(\frac{4\pi\sigma\ \cos\theta}{\lambda}\right)^2\right]\frac{G_X}{N_{RL}} \tag{6}$$

$$SNR_{RR} = P_{in}R_{RR}\exp\left[-\left(\frac{4\pi\sigma\ \cos\theta}{\lambda}\right)^2\right]\frac{G_X}{N_{RR}} \tag{7}$$

where $P_{in}$ is the incident signal power at the surface level, transmitted from GPS satellites. $G_R$ and $G_X$ are receiver antenna gains of coherent-polarization (RR) and cross-polarization (RL), respectively. $N_{sys}$, $N_{RR}$ and $N_{RL}$ are noise powers of direct, reflected signals in coherent-polarization and cross-polarization, respectively. Reflecting surfaces have a considerable roughness that contributes to the diffusion of reflected electromagnetic waves. The rough surface reflectance is related to specular surface reflectance ($R_{RR}$ and $R_{RL}$) and a small-scale roughness (σ) (Hong (2010a, 2010b)). According to a semi-empirical model of Ulaby et al. (1982), the

**Table 2.** Summary of GPS signal reflection experiments

| | Experimet A | Experimet A |
|---|---|---|
| Objective | Water dependency | Ice detection |
| Site | Ttukseom Han River Park, Seoul | Public service garage for trucks in Chuncheon |
| Date | November 16, 2016 | November 24, 2016 |
| Measurement duration | 45 min | 106 min |
| Air temperture/RH | 4.7°C/43% | -3.3°C/64% |
| Wind speend | 0.8 m/s | 1.3 m/s |
| Surface type | Soil | Asphalt |

degree of the reflection signal scattered by the rough surface can be expressed as follows (Hong, 2010a; 2010b):

$$R_{R,p} = R_p \exp\left[-\left(\frac{4\pi\sigma\ \cos\theta}{\lambda}\right)^2\right] \quad (8)$$

where $R_{R,p}$ and $R_p$ are the reflectance on the rough and specular surfaces for p-polarization (RR or RL), respectively. $\sigma$ is the standard deviation of the surface height of the height probability density function with a Gaussian distribution (Wu and Fung, 1972; Choudhury et al., 1979) corresponding to small-scale roughness. $\lambda$ is the observation wavelength and $\theta$ is the incident angle.

Estimation of the reflectance ($R_{RR}$ and $R_{RL}$) from observed SNR requires details about the incident signal power ($P_{in}$), received antenna gain ($G_R$ and $G_X$), noise power of the system ($N_{RR}$ and $N_{RL}$) and surface roughness information ($\sigma$). However, such information cannot be easily obtained. If we use the following Normalized Polarization Ratio Index (NPRI) equation, we can reduce some unknown variables of $P_{in}$ and roughness effect:

$$NPRI = \frac{SNR_{RR} - SNR_{RL}}{SNR_{RR} + SNR_{RL}} = \frac{R_{RR} - CR_{RL}}{R_{RR} + CR_{RL}} \quad (9)$$

where $C$ is a coefficient defined as $C = G_X / N_{RL} \cdot N_{RR} / G_R$, which is a function of the antenna gain and GPS receiver system. This coefficient should be determined by comparison with observation data. NPRI has the following advantages for black-ice detection: 1) NPRI values are restricted between −1 and 1. 2) NPRI is independent of small-scale surface roughness. 3) NPRI is independent of the signal power of direct GPS satellites. This means that only downward GPS antenna is required to determine the value of NPRI. The remaining unknown coefficient, $C$, can change with the elevation angle of the GPS satellite due to the elevation dependency of the antenna gain. Figure 3 illustrates the process of calculating NPRI from GPS signals obtained through the GPS receiver module.

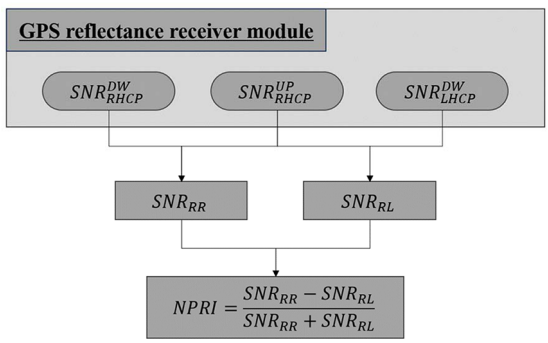


**Fig. 3.** Flow chart for calculating NPRI from GPS signals.

We measured the power of direct and reflected GPS L1 signals in experiment A and experiment B. In each experiment, the difference between *dSNR* for down-ward and upward antenna were calculated. The $dSNR_{RR}$ and $dSNR_{RL}$ corresponding reflectance, in dB, is simply defined as follows:

$$dSNR_{RR}(dB) = SNR_{RHCP} - SNR_{up} \propto R_{RR} \quad (10)$$

$$dSNR_{RL}(dB) = SNR_{LHCP} - SNR_{up} \propto R_{LR} \quad (11)$$

where $SNR_{up}$ is the SNR observed from the upward antenna to measure direct GPS signal strength, $SNR_{RHCP}$ and $SNR_{LHCP}$ are those observed from the down-ward antenna to measure the signal strengths of reflected RHCP and LHCP.

# 4. Results

## 4.1. Theoretical NPRI curves

Figure 4 shows the theoretical expectation of NPRI curves for water, ice, soil, and asphalt concrete. The NPRI values vary from 1 to −1 as the elevation angle of satellites increases. Within a certain elevation range, water surfaces can be distinguished from other surfaces using NPRI values. Although the difference between asphalt and ice surfaces is not large, we can easily determine whether the surface water is frozen.

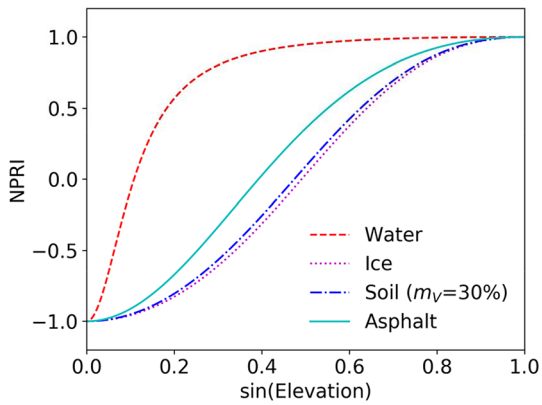


**Fig. 4.** Theoretical expectation of NPRI curves for water, ice, soil, and asphalt concrete surface.

## 4.2. Measurement of GPS

Figure 5 shows the time series of $dSNR_{RR}$ (blue line) and $dSNR_{RL}$ (red line) measured in experiments A and B, respectively. Experiment A was designed to identify changes in reflectivity in dry and wet soils. Because the refractive index of soil is similar with ice (Table 1), we can expect that the reflectivity contrast between water and ice surface is analogous to this experiment result. The black vertical dotted lines in Fig. 5 indicate the time lines during which water was sprayed on the soil. A clear difference was observed between the reflectivity of the dry and wet ground surfaces, as shown in PRN17 and PRN19 in Fig. 5.

In contrast, the signal strength remained unchanged between the reflected signals of dry ground surface in PRN06. This means that the reflectance change is caused by the higher moisture content of the soil. Experiment B was designed to observe the reflectivity difference between asphalt and ice surfaces.

Figure 5 displays the results of SNR measurements in experiment B. It shows distinct changes in $dSNR_{RR}$ and $dSNR_{RL}$ when the reflection surface changed between ice and asphalt. The weakening of reflectivity at some points might be due to deviation from the ice

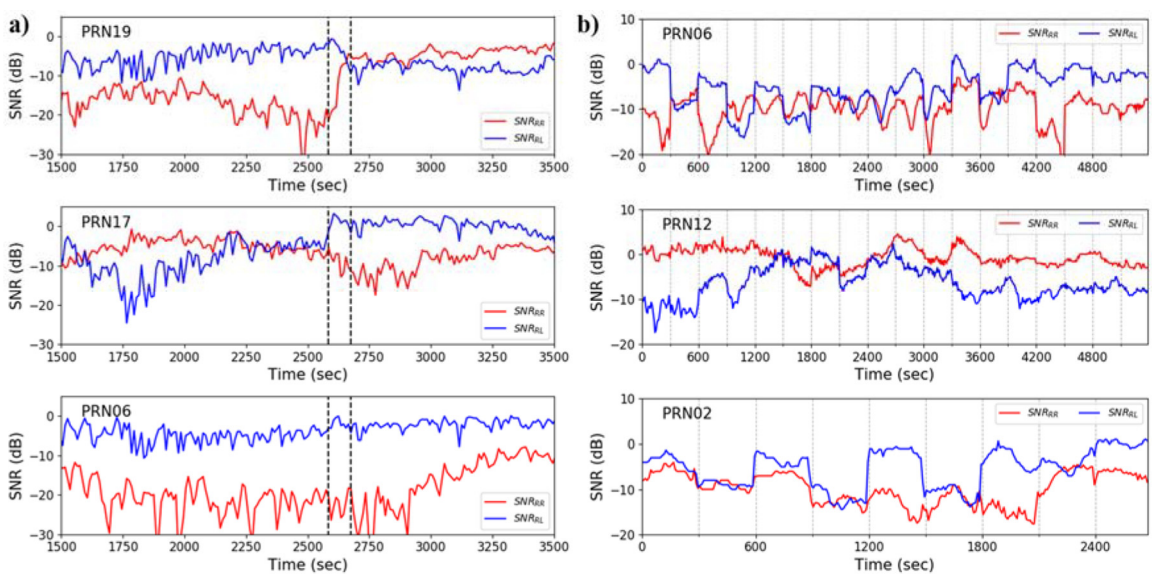


**Fig. 5.** Time series of SNRRR and SNRRL reflectance in experiment A (left three panels) and experiment B (right three panels).

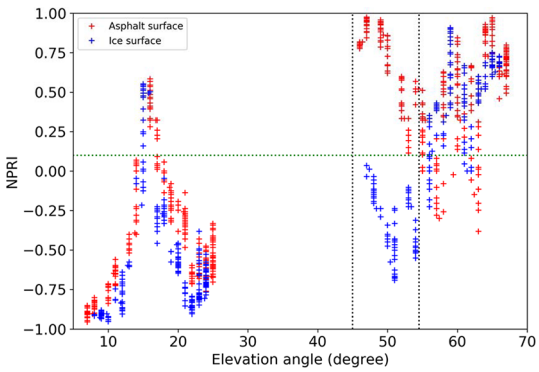


**Fig. 6.** NPRI dependency on the reflecting surface.

reflection plane. The $dSNR_{RR}$ and $dSNR_{RL}$ in experiments A and B show a large variation due to the change of surface reflectivity, surface roughness, antenna gain and surrounding noise level. Thus, the proposed NPRI might be more suitable parameter than *dSNR* because the NPRI is normalized within −1 to 1, and less sensitive to surface roughness than dSNR.

### 4.3. Interpretation of NPRI

Figure 6 shows a plot of NPRI values according to elevation angles from experiment B. The oscillating pattern in the low elevation angles can be analyzed as multipath effects (Larson and Nievinski, 2013; Jin and Najibi, 2014) that typically occur at low elevation angle. In this study, the details of patterns are not fully analyzed because we focused on the GPS signal processing at high elevation angles. At higher elevation angle regions, where the multipath effect is weakened, the NPRI values of asphalt and ice surfaces show a distinct difference, particularly noticeable between 45° and 55°. This result indicates that black-ice can be distinctly detectable with NPRI value less than 0.1 for the elevation angle between 45° and 55°.

The apparent difference in surface reflectivity and NPRI between the two experiments shows that GPS signals reflected off the ground can be used to distinguish between ice and water on asphalt. However, to improve the estimation accuracy, the roughness effect of the reflecting surface and the effect of multipaths such as elevation angle will be included as a future work.

## 5. Discussion

This study presents a novel approach to black ice detection using a GPS-based system that measures the signal strength of reflected GPS signals to estimate ground reflection components. By calculating the NPRI, we successfully distinguished between the reflective properties of water and ice on asphalt surfaces. The proposed GPS-based system offers several advantages: it is cost-effective, scalable, and capable of being integrated into existing GPS infrastructure. Unlike traditional infrared or optical sensors, the GPS-based system can monitor the sky day and night without relying on sunlight. These attributes make it a promising solution for large-scale black ice monitoring, potentially improving road safety in regions prone to freezing conditions. The system's ability to provide real-time, widespread detection could represent a significant advancement over traditional methods, often limited by high costs, sunlight interference, and narrow detection ranges.

As a preliminary study, the research was conducted under clear-sky conditions, representing a controlled environment. While the results are promising, the system's performance under more varied and challenging weather conditions, such as precipitation, fog, or heavy cloud cover, has yet to be explored. Additionally, the current study focused on a limited number of field sites, and further research is needed to assess the system's robustness and accuracy across diverse geographical areas and road surfaces. Future studies should aim to refine and validate the system under a broader range of environmental conditions, ensuring its reliability and effectiveness in real-world applications. Expanding the scope of testing will be crucial for fully realizing the potential of this GPS-based black ice detection system as a practical tool for enhancing winter road safety on a global scale.

## 6. Summary and Conclusions

In this paper, we proposed a new approach for the detection of black ice on pavements using reflected GPS signals. We developed a GPS signal measurement system (GPS antenna and receiver) to measure the power of GPS L1 band polarized signals. The field experiments in the two separate sites under different experimental conditions were performed using the developed GPS signal measurement system. As a result, the GPS signals reflected off a water surface behave differently from those reflected off soil. Furthermore, GPS signals reflected off an icy surface could be distinguished from those reflected off an asphalt surface. The proposed NPRI for black ice detection has advantages of its less sensitivity to small-scale surface roughness and independence on the direct GPS signal power. The results in this study showed that black ice was detectable using the GPS signal measurement system under the condition of NPRI <0.1 at the elevation angle between 45$^{o}$ and 55$^{o}$.

This study proposes the first application of GPS reflectance for black-ice detection. Weather conditions, such as clouds and precipitation, do not significantly affect L-band signals. This technique will aid in automatically providing information about water and ice on roads with low maintenance costs. Another advantage of this system is that the required data can be obtained over a wider range and distance than existing black ice detecting techniques, which use complex infrared cameras.

The multipath effect on the GPS signal power is required to improve the black-ice detection algorithm, allowing for more accurate information on current road conditions. Additionally, the accuracy of black-ice detection is expected to improve if auxiliary data, such as temperature and humidity, are incorporated into the analysis.

## Acknowledgments

This work was funded by the Korea Meteorological Administration Research and Development Program under Grant KMIPA2017-0040 and supported by a grant from the National Institute of Environment Research (NIER), funded by the Ministry of Environment (MOE) of the Republic of Korea (NIER-2024-01-02-035).

## References

Alimasi, N., Takahashi, S., and Enomoto, H., 2012, Development of a mobile optical system to detect road-freezing conditions. Bulletin of Glaciological Research, 30, 41-51.

Bevis, M., Businger, S., Herring, T.A., Rocken, C., Anthes, R.A., and Ware, R.H., 1992, GPS meteorology: Remote sensing of atmospheric water vapor using the Global Positioning System. Journal of Geophysical Research: Atmospheres, 97(D14), 15787-15801.

Chapman, L. and Thornes, J.E., 2011, What spatial resolution do we need for a route-based road weather decision support system?. Theoretical and Applied Climatology, 104, 551-559.

Choudhury, B.J., Schmugge, T.J., Chang, A., and Newton, R.W., 1979, Effect of surface roughness on the microwave emission from soils. Journal of Geophysical Research: Oceans, 84(C9), 5699-5706.

Choy, S., Wang, C.-S., Yeh, T.-K., Dawson, J., Jia, M., and Kuleshov, Y., 2015, Precipitable water vapor estimates in the Australian region from ground-based GPS observations. Advances in Meteorology, 2015(1), 956481.

Dobson, M.C., Ulaby, F.T., Hallikainen, M.T., and El-Rayes, M.A., 1985, Microwave dielectric behavior of wet soil-part II: Dielectric mixing models. IEEE Transactions on Geoscience and Remote Sensing, GE-23(1), 35-46.

Evans, S.G., Small, E.E., and Larson, K.M., 2014, Comparison of vegetation phenology in the Western USA determined from reflected GPS microwave signals and NDVI. International Journal of Remote Sensing, 35(9), 2996-3017.

Hong, S., 2009, Retrieval of refractive index over specular surfaces for remote sensing applications. Journal of Applied Remote Sensing, 3(1), 033560.

Hong, S., 2010a, Surface roughness and polarization ratio in microwave remote sensing. International Journal of Remote Sensing, 31(10), 2709-2716.

Hong, S., 2010b, Global retrieval of small-scale roughness over land surfaces at microwave frequency. Journal of Hydrology, 389(1-2), 121-126.

Hong, S., 2013, Polarization conversion for specular components of surface reflection, IEEE Geoscience and Remote Sensing Letters, 10(6), 1469-1472.

Hufford, G., 1991, A model for the complex permittivity of ice at frequencies below 1 THz. International Journal of

Infrared and Millimeter Waves, 12, 677-682.

Jin, S. and Najibi, N., 2014, Sensing snow height and surface temperature variations in Greenland from GPS reflected signals. Advances in Space Research, 53(11), 1623-1633.

Johnson, B.T., Petty, G.W., and Skofronick-Jackson, G., 2012, Microwave properties of ice-phase hydrometeors for radar and radiometers: Sensitivity to model assumptions. Journal of Applied Meteorology and Climatology, 51(12), 2152-2171.

Jonsson, P., 2011, Remote sensor for winter road surface status detection, In. Proc. SENSORS, 2011 IEEE, 1285-1288.

Koch, F., Schlenz, F., Prasch, M., Appel, F., Ruf, T., and Mauser, W., 2016, Soil moisture retrieval based on GPS signal strength attenuation. Water, 8(7), 276.

Komjathy, A., Maslanik, J., Zavorotny, V.U., Axelrad, P., and Katzberg, S.J., 2000, Sea ice remote sensing using surface reflected GPS signals, In. Proc. IEEE 2000 International Geoscience and Remote Sensing Symposium (IGARSS 2000). Taking the Pulse of the Planet: The Role of Remote Sensing in Managing the Environment, 2855-2857.

Larson, K.M., 2016, GPS interferometric reflectometry: Applications to surface soil moisture, snow depth, and vegetation water content in the Western United States. Wiley Interdisciplinary Reviews: Water, 3(6), 775-787.

Larson, K.M. and Nievinski, F.G., 2013, GPS snow sensing: Results from the Earthscope plate boundary observatory. GPS Solutions, 17, 41-52.

Larson, K.M. and Small, E.E., 2014, Normalized microwave reflection index: A vegetation measurement derived from GPS networks. IEEE Journal of Selected Topics in Applied Earth Observations and Remote Sensing, 7(5), 1501-1511.

Larson, K.M., Gutmann, E.D., Zavorotny, V.U., Braun, J.J., Williams, M.W., and Nievinski, F.G., 2009, Can we measure snow depth with GPS receivers?. Geophysical Research Letters, 36(17), L17502.

Larson, K.M., Small, E.E., Gutmann, E., Bilich, A., Axelrad, P., and Braun, J., 2008, Using GPS multipath to measure soil moisture fluctuations: Initial results. GPS Solutions, 12, 173-177.

Liu, T., Pan, Q., Sanchez, J., Sun, S., Wang, N., and Yu, H., 2017, Prototype decision support system for black ice detection and road closure control. IEEE Intelligent Transportation Systems Magazine, 9(2), 91-102.

Ma, X. and Ruan, C., 2020, Method for black ice detection on roads using tri-wavelength backscattering measurements. Applied Optics, 59(24), 7242-7246.

Mahoney III, W.P. and Myers, W.L., 2003, Predicting weather and road conditions: Integrated decision-support tool for winter road-maintenance operations. Transportation Research Record, 1824(1), 98-105.

Najafi, M., Gorgin, S., Fallah, M.K., Jaberipur, G., and Lee, J.A., 2024, Low-power black-ice detection for safety critical edge devices on roads, In. Proc. 2024 Fifteenth International Conference on Ubiquitous and Future Networks (ICUFN), 636-641.

Nakanishi, Y. and Kushihi, Y., 2021, U.S. Patent Application No. 16/647,046.

Njoku, E.G. and Entekhabi, D., 1996, Passive microwave remote sensing of soil moisture. Journal of Hydrology, 184(1-2), 101-129.

Norrman, J., Eriksson, M., and Lindqvist, S., 2000, Relationships between road slipperiness, traffic accident risk and winter road maintenance activity. Climate Research, 15(3), 185-193.

Parkinson, B.W. and Spilker, J.J., 1996, Global Positioning System: Theory and applications, volume I. In Parkinson, B.W. (ed.), Introduction and heritage of Navstar, the global positioning system. progress in astronautics and aeronautics No. 163, American Institute of Aeronautics and Astronautics, Inc., Washington, DC, USA, 11.

Pilli-Sihvola, Y., Toivonen, K., Haavasoja, T., Haavisto, V., and Nylander, P., 2006, New approach to road weather: Measuring slipperiness, In. Proc. The 13th Standing International Road Weather Commission (SIRWEC) conference, 13-18.

Piuzzi, E., Cannazza, G., Cataldo, A., Chicarella, S., De Benedetto, E., Frezza, F., Pisa, S., Prontera, S., and Timpani, F., 2015, Measurement system for evaluating dielectric permittivity of granular materials in the 1.7-2.6-GHz band. IEEE Transactions on Instrumentation and Measurement, 65(5), 1051-1059.

Stogryn, A., 1971,. Equations for calculating the dielectric constant of saline water (correspondence). IEEE Transactions on Microwave Theory and Techniques, 19(8), 733-736.

Ulaby, F.T., Moore, R.K., and Fung, A.K., 1982, Microwave remote sensing: active and passive. Volume 2 - radar remote sensing and surface scattering and emission theory.

Wu, S.T. and Fung, A.K., 1972, A noncoherent model for microwave emissions and backscattering from the sea surface. Journal of Geophysical Research, 77(30), 5917-5929.

Zavorotny, V.U. and Voronovich, A.G., 2000, Scattering of GPS signals from the ocean with wind remote sensing application. IEEE Transactions on Geoscience and Remote Sensing, 38(2), 951-964.

Manuscript received: July 22, 2024
Revised manuscript received: August 27, 2024
Manuscript accepted: August 29, 2024